

Yashna Anthony*, Veena Ragupathi

Centre of Clean Energy and Nanoconvergence (CENCON), Department of Chemistry, Hindustan Institute of Technology and Science, Padur, Chennai, India

Scientific paper

ISSN 0351-9465, E-ISSN 2466-2585

<https://doi.org/10.62638/ZasMat1002>



Zastita Materijala 65 (1)
151 - 157 (2024)

Superior electrochemical performance of SnSe-PPy nanocomposites for supercapacitor application

ABSTRACT

Recently, Metal chalcogenides have received considerable interest in the field of energy storage devices. In this work, tin selenide-polypyrrole (SnSe-PPy) nanocomposite has been synthesized by hydrothermal method and its supercapacitive behavior is investigated. The synthesized SnSe-PPy nanocomposite is analysed by X-ray diffraction (XRD), Fourier transform infrared spectroscopy (FTIR), Scanning electron microscopy (SEM) and electrochemical characterisation. XRD confirms the existence of orthorhombic SnSe, and the FTIR result reveals the presence of polypyrrole. The supercapacitive behavior of SnSe-PPy nanocomposite is studied by cyclic voltammetry and galvanostatic charge-discharge studies. SnSe-PPy nanocomposite delivers the specific capacitance of 223 F g^{-1} at 10 mV sec^{-1} . The addition of polypyrrole increases the conductivity of the material and improves its supercapacitive behavior.

Keywords: Tin selenide, polypyrrole, supercapacitor, specific capacity, cycle life

1. INTRODUCTION

The global economy is severely affected by energy crises and environmental degradation problems. Energy production mainly depends on the combustion of fossil fuels, which produce greenhouse gas emissions and pollution. Therefore, generating effective storage devices that produce clean and sustainable energy is essential. In this perspective, batteries, fuel cells, and supercapacitors are effectively utilized as electrochemical energy storage devices [1,2]. In batteries, chemical energy is converted into electrical energy through a process called a redox reaction. Fuel cells work similar to batteries, but chemical energy from fuel is converted into electrical energy. In this context, a supercapacitor (SC) is a promising energy storage device that fills the gap between conventional capacitors and batteries [3,4]. SCs provide higher power outputs than batteries and store more energy than capacitors.

Benefiting from the better characteristics of supercapacitors such as high power density and

long-term stability, it is extensively used in electric motors, wind turbines, MP3 players and Regenerative braking [5,6]. Mostly, Supercapacitors are used alone or in conjunction with other energy storage technology [7-9]. In supercapacitors, the electrode stores charges by the non-faradic and faradaic processes. Supercapacitors are classified into four types: (i) electrolytic double layer (EDLC), (ii) pseudo, (iii) hybrid and (iv) battery-type capacitors [10]. Among all, the pseudo supercapacitors have gained significant attention due to their exceptional features like high power density and enhanced cycle life.

Generally, using appropriate electrode materials with nanostructured architecture improves the electrochemical performance and efficiency of SCs [11,12]. The electrode material can be made from a variety of materials [12]. Carbon-based materials are used in EDLCs and transition metal oxides (RuO_2 , TiO_2 , ZnO , GeO_2), metal chalcogenides (SnS , MoS_2 , WS_2 , MoSe), conducting polymers (polyaniline (PANI), polypyrrole (PPy), polyacetylene (PA), polythiophene (PTH)) are used in Pseudo-capacitors [13-15].

In recent years, Metal chalcogenides have drawn significant interest, and tin selenides (SnSe) is gaining popularity due to their diverse application like thermoelectric, sensors, solar cells, and energy storage [16-18]. Manoj Kumar et al. reviewed the

*Corresponding author: Yashna Anthony

E-mail: rveena@hindustanuniv.ac.in

Paper received: 28. 09. 2023.

Paper accepted: 27. 11. 2023.

Paper is available on the website: www.idk.org.rs/journal

physical properties of tin-selenide material, such as phases, defects, growth mechanisms, deposition methods, and the various possible applications. Due to their favourable bandgap and absorption coefficient, these materials have gained significant attention in photovoltaic and optoelectronic applications [19]. However, among other metal chalcogenides, very few works have been published on the supercapacitive behavior of SnSe. Zhang et al. fabricated 2D, tin selenide nanodisks and nanosheets, and SnSe nanodisk delivered the specific capacitances of 168 F g^{-1} , and SnSe nanosheet yielded 228 F g^{-1} [20]. In general, the addition of conducting polymers, especially Polypyrrole (PPy), improves the electrochemical performance of metal chalcogenides by the providing necessary surface area, which improves the charge storage capacity. Yang Huang et al. demonstrated various synthesis procedures to fabricate PPy nanostructures [21]. Polypyrrole has promising properties such as high conductivity, stability, large surface area, and low equivalent series resistance, and these properties are essential to fabricating efficient supercapacitors.

Hence, in this study, to enhance the electrochemical performance of tin selenide, polypyrrole is incorporated, and SnSe-PPy nanocomposites have been prepared using a hydrothermal method. The supercapacitive behavior of SnSe-PPy nanocomposites is investigated.

2. MATERIALS AND METHODS

2.1. Materials

Tin (II) chloride dihydrate ($\text{SnCl}_2 \cdot 2\text{H}_2\text{O}$) was purchased from Merck Life Science Private Limited Mumbai. Selenium, pyrrole, hydrogen hydrazine,

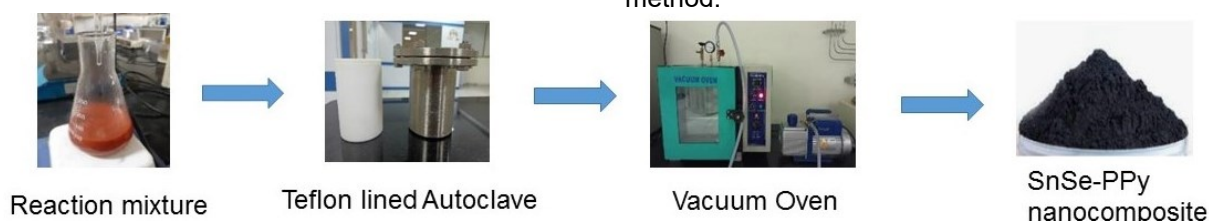


Figure 1. Synthesis of SnSe-PPy nanocomposite

Slika 1. Sinteza SnSe-PPi nanokompozita

2.4. Characterizations

The X-ray diffraction (XRD) characterization was carried out using an X-ray diffractometer (BRUKER USA D8 Advance, Davinci). Fourier transform infrared spectroscopy (FTIR) measurements were performed using Nicolet iS50 within the operating range of $400\text{--}4000 \text{ cm}^{-1}$. The FTIR sample is prepared by adding 200 mg of anhydrous potassium bromide with 2 mg of the

potassium hydroxide, Sodium hydroxide pellets, and ethanol were purchased from Sigma Aldrich.

2.2. Synthesis of Polypyrrole (PPy)

The synthesis of polypyrrole (PPy) was carried out using the chemical polymerization method. 3 g of dodecyl benzene sulphonic acid (50 ml) was added to the 0.1 M ferric chloride solution (50 ml). Following this, 0.1 M of pyrrole was added dropwise to the mixed solution at 5°C for 4 h. After the polymerization process was complete, the obtained polypyrrole was washed with distilled water to remove residual reactants and by-products. Finally, the washed PPy was dried at 60°C to get the final PPy material. This process involves the formation of a polymer from a monomer, where the monomer pyrrole underwent oxidative polymerization in the presence of a dopant, dodecyl benzene sulphonic acid, and an oxidant, ferric chloride hexahydrate.

2.3. Synthesis of SnSe-PPy nanocomposite

The hydrothermal method was adopted to synthesize SnSe-PPy nanocomposite materials. To synthesize SnSe-PPy nanocomposites, 2.6 grams of $\text{SnCl}_2 \cdot \text{H}_2\text{O}$, 0.1 grams of selenium and 10 wt% polypyrrole were added to 100 ml of distilled water and stirred at room temperature for 2 h. Then, the NaOH (0.01M) solution, followed by hydrogen hydride solutions, was added to the precursor's solution and stirred for 6h. The solution was transferred to an autoclave and heated at 100°C for 8 h. The resulting blackish-brown colour solution was centrifuged at 3000 RPM. At last, the powder was washed with distilled water and dried at 60°C in the oven. Fig. 1 represents the synthesis of SnSe-PPy nanocomposite by hydrothermal method.

sample. Then the mixture was pelletized with a pressure of 10 k Pa cm^2 . The morphology of the material was analysed using a VEGA3 TESCAN scanning electron microscope.

2.4.1. Electrochemical Characterization

The electrochemical characterizations were carried out using a VersSTAT-3 electrochemical workstation. The three-electrode configuration is

used to perform the supercapacitive behavior of SnSe-PPy nanocomposite. The working electrodes were prepared by mixing an 80:10:10 ratio of active material, carbon black and polyvinylidene difluoride (PVDF) respectively. The slurry was then coated onto a stainless steel current collector with a 1x1 cm² area and dried overnight at 90°C. The weight of the electrode material coated on the SS electrode was kept constant at approximately 1mg for all electrochemical measurements. Pt foil and

Ag/AgCl were used as a counter and reference electrode. 2M KOH solution was used as an electrolyte.

3. RESULT AND DISCUSSIONS

X-ray diffraction pattern of pure PPy is shown in Fig. 2a, and the result reveals a broad pattern in the range $2\theta = 20^\circ$ and 30° , which indicates the formation of amorphous PPy [22].

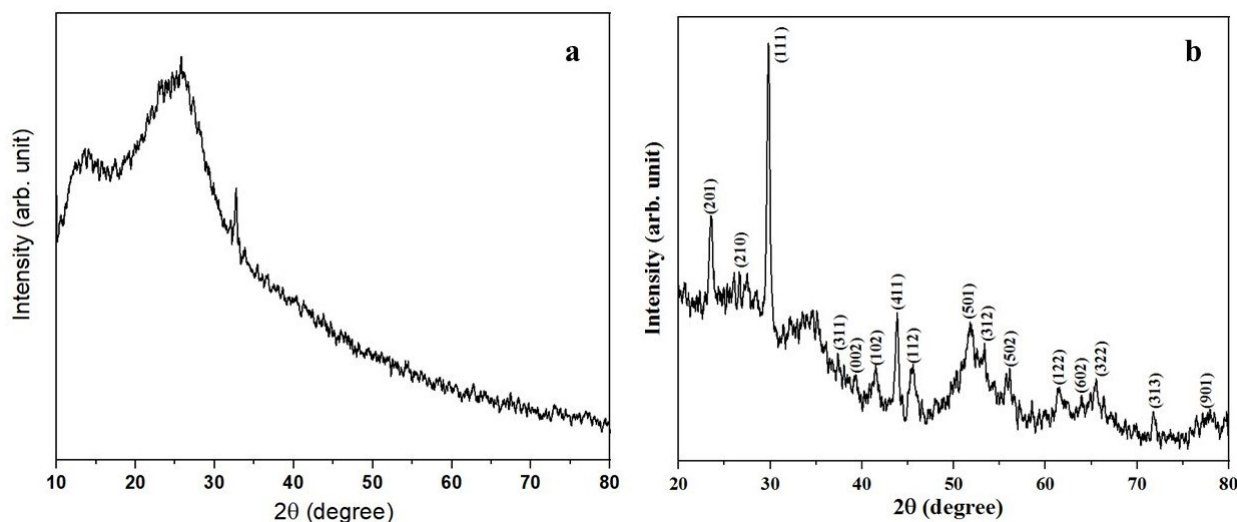


Figure 2. (a&b) XRD diffraction pattern of polypyrrole (PPy) and SnSe-PPy nanocomposite

Slika 2. (a&b) XRD difrakcioni uzorak polipirola (PPi) i nanokompozita SnSe-PPi

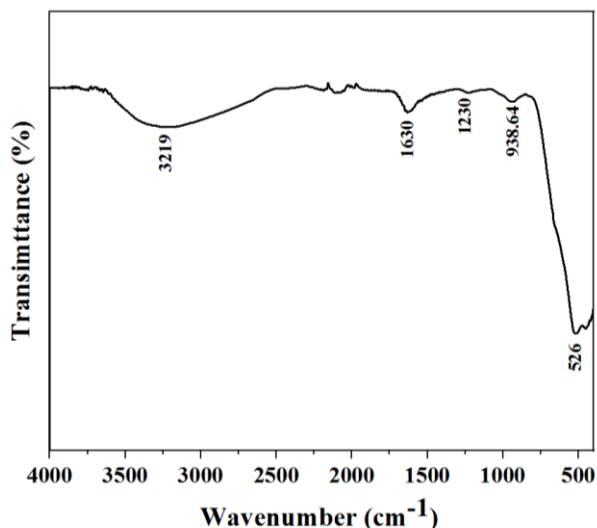


Figure 3. FTIR spectrum of SnSe-PPy nanocomposite

Slika 3. FTIR spektar SnSe-PPi nanokompozita

Fig. 2b reveals the XRD pattern of hydrothermal-derived SnSe-PPy materials. The X-ray diffraction pattern exhibits two theta peaks at 23.41° , 30.12° , 41.54° , 51.67° , 65.38° , and 61.46°

corresponding to the (201), (111), (102), (601), (203), and (122) planes respectively. The XRD results confirm the existence of the orthorhombic phase of SnSe. The lattice parameter values 'a', 'b', and 'c' were calculated and are found to be $a = 11.057 \text{ \AA}$, $b = 4.164 \text{ \AA}$, $c = 4.604 \text{ \AA}$ which is well matched with the JCPDS data (89-0236). No predominant peak corresponding to polypyrrole was observed.

The chemical structures of SnSe-PPy nanocomposite were studied by the FTIR technique. FTIR Spectra of SnSe-PPy material are shown in Fig. 3. The peak that appeared at 526 cm^{-1} corresponds to SnSe vibration. The characteristic peak of polypyrrole is observed at 1630 cm^{-1} , 939 cm^{-1} , 1230 cm^{-1} and 3219 cm^{-1} . The peak at 1630 cm^{-1} attributes C=C vibration modes. The peaks at 939 and 1230 cm^{-1} ascribe to C-H wagging and C-N bonds, respectively. The occurrence of the broad peak at 3219 cm^{-1} is attributed to N-H stretching vibrations in the pyrrole ring [23].

The electrochemical properties of electrode materials are significantly influenced by their surface morphology and specific surface area. The size and shape of the SnSe-PPy material were analyzed by scanning electron microscope.

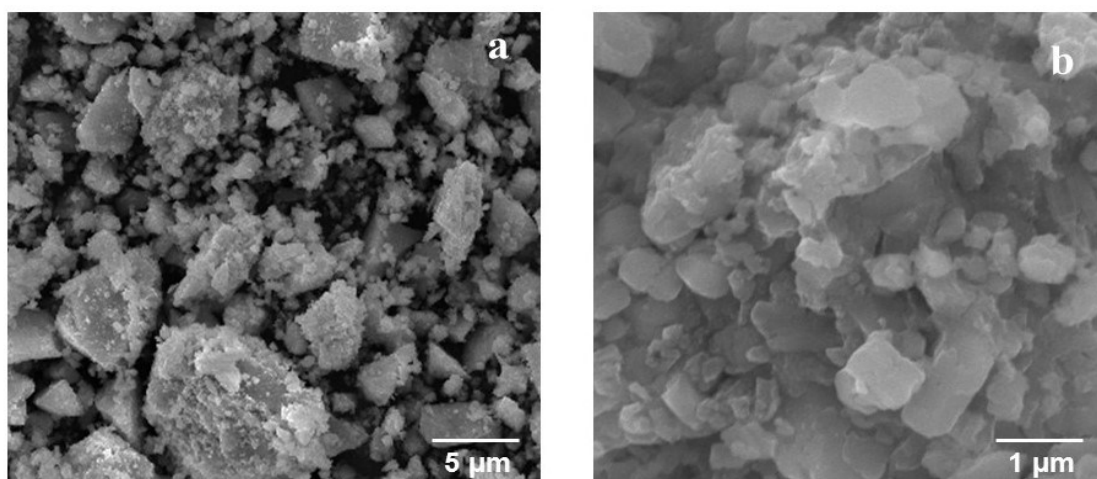


Figure 4. (a & b) SEM images of SnSe-PPy nanocomposite

Slika 4. (a i b) SEM slike SnSe-PPi nanokompozita

The morphology of SnSe-PPy nanoparticles was recorded using SEM, and the images are shown in Fig. 4 (a & b). The magnified SEM image (Fig. 4b) illustrates the presence of agglomerated triangle and spherical shape particles with an average size of 100 nm to 500 nm.

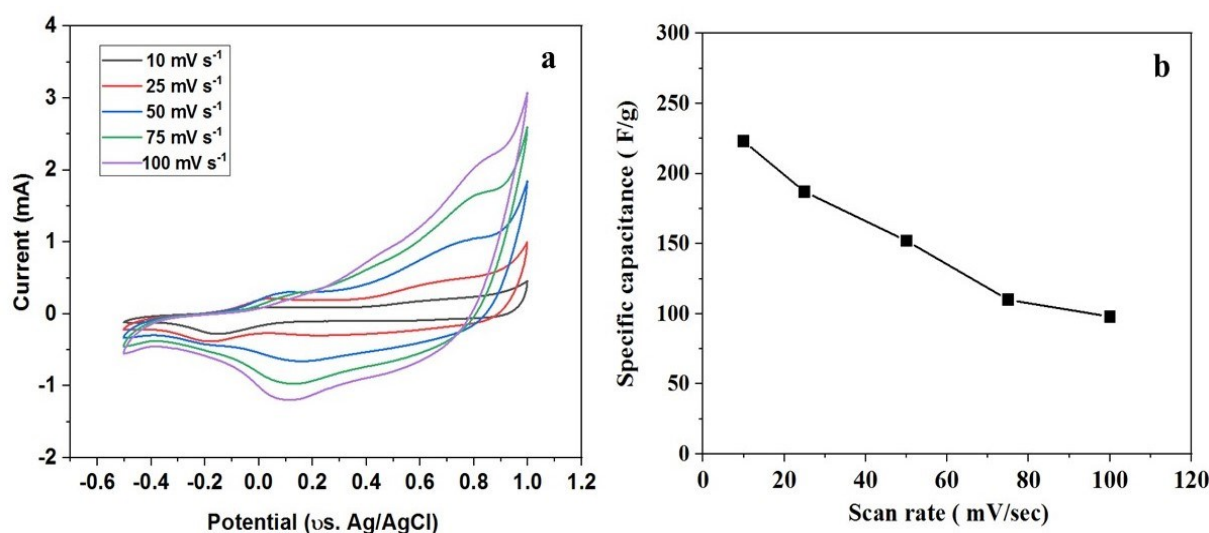


Figure 5. a) Cyclic voltammogram and b) specific capacitance versus scan rate

Slika 5. a) Ciklični voltamogram i b) specifična kapacitivnost u odnosu na brzinu skeniranja

The Cyclic Voltammetry (CV) technique is utilized to investigate the redox properties and reversibility of SnSe-PPy nanocomposites as shown in Fig. 5a. The CV measurements were performed at the scan rates of 10, 25, 50, 75, and 100 mV s^{-1} and potential window of -0.4 V to 1 V. The negative and positive current regions detected in the CV curves indicate the cathodic reduction and anodic oxidation processes. The CV result confirms the existence of reversible reaction ($\text{Sn}^{2+} \leftrightarrow \text{Sn}^{4+}$) in SnSe-PPy nanocomposites [20]. The CV results exhibit the faradaic behavior of SnSe-PPy material.

The increase of integral current area shows the enhancement of the capacitive behavior of SnSe-PPy electrodes. When the scan rate increases, the area under the CV curve also increases, indicating that there is an outstanding capacitive behavior [24].

The equations below were used to calculate the special capacitance of SnSe-PPy electrodes.

$$C_s = \frac{\int I dt}{m\theta}$$

where

C_s is the specific capacitance of the SnSe-PPy electrodes

m is the amount of active material,

ϑ is the scan rate and I is the Integral current.

The calculated specific capacitance values are 223, 187, 152, 110 and 98 F g⁻¹ at the scan rates of

10, 25, 50, 75 and 100 mV s⁻¹ respectively (Fig. 5b). At a scan rate of 10 mV s⁻¹, an exceptionally high capacitance of 223 F g⁻¹ was observed. However, at faster scan rates, only the material's outer surface can participate in the capacitive process with the electrolyte ions, leading to less utilization of the electroactive material.

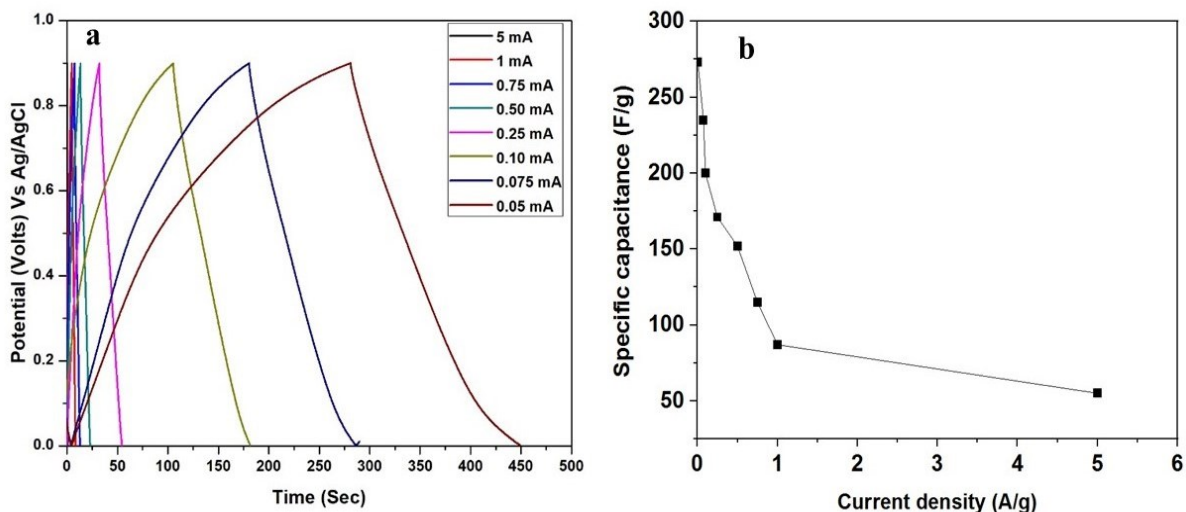


Figure 6. a) Galvanostatic charge discharge measurements, b) Specific capacitance versus current densities

Slika 6. a) Merenja galvanostatskog pražnjenja, b) Specifični kapacitet u odnosu na gustinu struje

Fig. 6a shows the galvanostatic charge-discharge (GCD) curves for SnSe-PPy nanocomposite electrodes at different current densities. The specific capacitance C_s is calculated from the GCD curve using the following equation,

$$C_s = \frac{I\Delta t}{m\Delta V}$$

The specific capacitance versus current densities is shown in the Fig. 6b. The calculated specific capacitance at different current densities of 0.05, 0.075, 0.10, 0.25, 0.50, 0.75, 1 and 5 mA are 273, 235, 200, 171, 152, 115, 87 and 55 F g⁻¹ respectively.

At a current density of 0.05 mA, the electrode exhibits a maximum specific capacitance of 273 F g⁻¹. It is usual for supercapacitors to experience a reduction in capacitance at relatively higher current densities due to the faster discharge rate compared to lower current densities [25]. The incorporation of polypyrrole enhances the electrical conductivity and improves the electrochemical performance of SnSe-PPy nanocomposite.

Electrochemical impedance spectra of the SnSe-PPy electrode are measured in the range of 100 kHz to 0.01 Hz and shown in Fig. 7. The semicircle at a high frequency range indicates the charge transfer process at the electrode -

electrolyte interface. On the Nyquist plot, the point where the semicircle intersects the real axis shows the solution resistance (R_s) and charge transfer resistance (R_{ct}) [26,27].

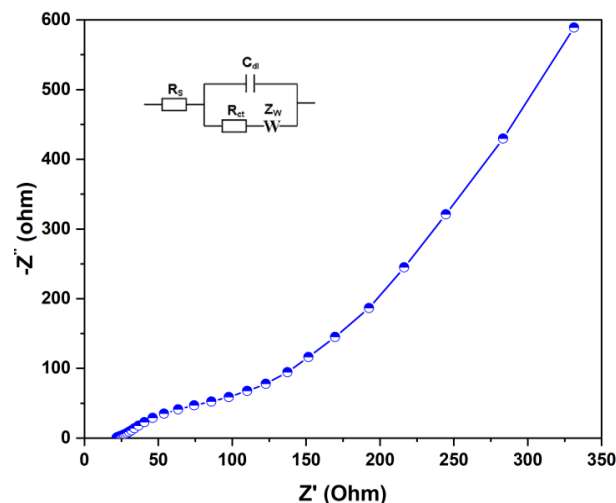


Figure 7. Nyquist plot of SnSe-PPy electrode

Slika 7. Nyquist-ov dijagram SnSe-PPi elektrode

The inset Fig. 7 displays the equivalent circuit diagram (Randle circuit). The diagonal line in the low-frequency range denotes Warburg impedance, which is associated with the diffusion of ions from the electrolyte to the surface of the electrode. The

Nyquist plot shows a straight line in the low-frequency area and a quasi-semicircle in the high-frequency region. These patterns are related to the mass transfer and charge transfer processes, respectively.

The equivalent circuit comprises various parameters, including the bulk resistance (R_s), charge transfer resistance (R_{ct}), C_{dl} , which denotes the pseudo capacitance, and Warburg parameter (W). The solution resistance (R_s) is 21 Ω , and the charge transfer resistance (R_{ct}) is 46.25 Ω .

4. CONCLUSIONS

In this work, SnSe-PPy nanocomposites are synthesized by the hydrothermal method and the supercapacitive behavior of SnSe-PPy nanocomposites is investigated. XRD confirms the formation of orthorhombic SnSe. The SEM image shows agglomerated triangle-shaped particles. The SnSe-PPy electrode delivers the specific capacitance of 273 Fg^{-1} at 0.05 mA. The incorporation of polypyrrole enhances the electrical conduction and improves the electrochemical performance of SnSe-PPy nanocomposite. However, scalable synthesis and optimization of polypyrrole quantity has been required for commercial application.

Acknowledgements

Veena Ragupathi acknowledges the research funding from the Science and Engineering Research Board (SERB), Govt. of India under TARE – SERB (No.TAR/2019/000125).

5. REFERENCES

- [1] A. Dutta, S. Mitra, M. Basak, T. Banerjee (2023) A comprehensive review on batteries and supercapacitors: Development and challenges since their inception, *Energy Storage.*, 5, e339.
- [2] S. Badwal, S. Giddey, C. Munnings, A. Bhatt, A. Hollenkamp (2014) Emerging electrochemical energy conversion and storage technologies, *Front. Chem.*, 2, 79, 1-28.
- [3] W. Zuo, R. Li, C. Zhou, Y. Li, J. Xia, J. Liu (2017) Battery-Supercapacitor Hybrid Devices: Recent Progress and Future Prospects, *Adv. Sci.*, 4, 1600539, 1-29.
- [4] M. Winter, R.J. Brodd (2004) What Are Batteries, Fuel Cells, and Supercapacitors?, *Chem. Rev.*, 104, 4245-4270.
- [5] V. Ragupathi, P. Panigrahi, G.S. Nagarajan (2023) Review—Supercapacitor Active Material from Recycling, *ECS J. Solid State Sci. Technol.*, 12, 24001.
- [6] M.E. Şahin, F. Blaabjerg, A. Sangwongwanich (2022) A Comprehensive Review on Supercapacitor Applications and Developments, *Energies.*, 15, 674, <https://doi.org/10.3390/en15030674>
- [7] S.M. Benoy, M. Pandey, D. Bhattacharjya, B.K. Saikia (2022) Recent trends in supercapacitor-battery hybrid energy storage devices based on carbon materials, *J. Energy Storage.*, 52, 104938.
- [8] A. Townsend, C. Martinson, R. Gouws, D. Bessarabov (2021) Effect of supercapacitors on the operation of an air-cooled hydrogen fuel cell, *Heliyon.*, 7, e06569.
- [9] Q. Xun, S. Lundberg, Y. Liu (2021) Design and experimental verification of a fuel cell/supercapacitor passive configuration for a light vehicle, *J. Energy Storage.*, 33, 102110. <https://doi.org/10.1016/j.est.2020.102110>
- [10] M.A. Mohd Abdah, N.H.N. Azman, S. Kulandaivalu, Y. Sulaiman (2019) Review of the use of transition-metal-oxide and conducting polymer-based fibres for high-performance supercapacitors, *Mater. Des.*, 186, 108199. <https://doi.org/10.1016/j.matdes.2019.108199>
- [11] B.K. Saikia, S.M. Benoy, M. Bora, J. Tamuly, M. Pandey, D. Bhattacharya (2020) A brief review on supercapacitor energy storage devices and utilization of natural carbon resources as their electrode materials, *Fuel.*, 282, 118796.
- [12] S. Rajagopal, R.M. Ibrahim, D. Velez (2022) Electrode Materials for Supercapacitors in Hybrid Electric Vehicles: Challenges and Current Progress, *Condens. Matter.*, 7, 6, 1-33.
- [13] Z.S. Iro, C. Subramani, S.S. Dash (2016) A Brief Review on Electrode Materials for Supercapacitor, *Int. J. Electrochem. Sci.*, 11, 10628-10643, doi: 10.20964/2016.12.50
- [14] M.Z. Ansari, S.A. Ansari, S.-H. Kim (2022) Fundamentals and recent progress of Sn-based electrode materials for supercapacitors: A comprehensive review, *J. Energy Storage.*, 53, 105187.
- [15] M. Vandana, S. Veeresh, H. Ganesh, Y.S. Nagaraju, H. Vijeth, M. Basappa, H. Devendrappa (2022) Graphene oxide decorated SnO₂ quantum dots/polypyrrole ternary composites towards symmetric supercapacitor application, *J. Energy Storage.*, 46, 103904.
- [16] W. Shi, M. Gao, J. Wei, J. Gao, C. Fan, E. Ashalley, H. Li, Z. Wang (2018) Tin Selenide (SnSe): Growth, Properties, and Applications, *Adv. Sci.*, 5, 1700602.
- [17] M.R. Burton, S. Mehraban, D. Beynon, J. McGettrick, T. Watson, N.P. Lavery, M.J. Carnie (2019) 3D Printed SnSe Thermoelectric Generators with High Figure of Merit, *Adv. Energy Mater.*, 9, 1900201.
- [18] J. Kang, L. Wang, L. Zhang (2023) Discrete card-shaped bimetallic selenides as anode materials for sodium ion batteries with excellent long cycle stability, *J. Solid State Chem.*, 323, 124014.
- [19] M. Kumar, S. Rani, Y. Singh, K. Gour, V.N. Singh (2021) Tin-selenide as a futuristic material: properties and applications, *RSC Adv.*, 11, 6477.
- [20] C. Zhang, H. Yin, M. Han, Z. Dai, H. Pang, Y. Zheng, Y.-Q. Lan, J. Bao, J. Zhu (2014) Two-

- Dimensional Tin Selenide Nanostructures for Flexible All-Solid-State Supercapacitors, ACS Nano., 8, 3761.
- [21] Y. Shi, L. Pan, B. Liu, Y. Wang, Y. Cui, Z. Bao, G. Yu (2014) Nanostructured conductive polypyrrole hydrogels as high-performance, flexible supercapacitor electrodes, J. Mater. Chem. A., 2, 6086-6091.
- [22] S. Shrikrushna, J. Kulkarni (2015) Influence of Dodecylbenzene Sulfonic Acid Doping on Structural, Morphological, Electrical and Optical Properties on Polypyrrole/3C-SiC Nanocomposites, J. Nanomed. Nanotechnol., 6, 5, 1000313.
- [23] M.U. Shariq, A. Husain, M. Khan, A. Ahmad (2021) Synthesis and characterization of polypyrrole/molybdenum oxide composite for ammonia vapour sensing at room temperature, Polym. Polym. Compos., 29, S989.
- [24] B. Pandit, L.K. Bommineedi, B.R. Sankapal (2019) Electrochemical engineering approach of high performance solid-state flexible supercapacitor device based on chemically synthesized VS2 nanoregime structure, J. Energy Chem., 31, 79-88.
- [25] C. Tian, Q. Lu, S. Zhao (2019) Monodispersed and hierarchical silica@manganese silicate core-shell spheres as potential electrodes for supercapacitor, J. Solid State Chem., 277, 475-483. <https://doi.org/10.1016/j.jssc.2019.07.006>
- [26] B. Pandit, B. Sankapal, P. Koinkar (2019) Novel chemical route for CeO2/MWCNTs composite towards highly bendable solid-state supercapacitor device, Sci. Rep., 9, 5892-5905. doi: 10.1038/s41598-019-42301-y
- [27] B. Pandit, C.D. Jadhav, P.G. Chavan, H.S. Tarkas, J. V Sali, R.B. Gupta, B.R. Sankapal (2020), Two-Dimensional Hexagonal SnSe Nanosheets as Binder-Free Electrode Material for High-Performance Supercapacitors, IEEE Trans. Power Electron., 35, 11344-11351. doi: 10.1109/TPEL.2020.2989097

IZVOD

SUPERIORNE ELEKTROHEMIJSKE PERFORMANSE SNSE-PPY NANOKOMPOZITA ZA PRIMENU U SUPERKONDENZATORIMA

Nedavno su metalni halkogenidi dobili značajno interesovanje u oblasti uređaja za skladištenje energije. U ovom radu hidrotermalnom metodom je sintetizovan nanokompozit kalaj selenid-polipirol (SnSe-PPi) i ispitano je njegovo superkapacitivno ponašanje. Sintetizovani SnSe-PPi nanokompozit je analiziran rendgenskom difrakcijom (XRD), infracrvenom spektroskopijom Furijeove transformacije (FTIR), skenirajućom elektronskom mikroskopom (SEM) i elektrohemijom karakterizacijom. XRD potvrđuje postojanje ortorombičnog SnSe, a FTIR rezultat otkriva prisustvo polipirola. Superkapacitivno ponašanje SnSe-PPi nanokompozita je proučavano cikličnom voltametrijom i studijama galvanostatskog pražnjenja. SnSe-PPi nanokompozit isporučuje specifičan kapacitet od 223 F g^{-1} pri 10 mV sec^{-1} . Dodatak polipirola povećava provodljivost materijala i poboljšava njegovo superkapacitivno ponašanje.

Ključne reči: Kalaj selenid, polipirol, superkondenzator, specifični kapacitet, životni vek.

Naučni rad

Rad primljen: 28.09.2023.

Rad prihvaćen: 27.11.2023.

Rad je dostupan na sajtu: www.idk.org.rs/casopis